


***Ab initio* electronic stationary states for nuclear projectiles in solids**Jessica F. K. Halliday ¹, Marjan Famili,¹ Nicolò Forcellini ², and Emilio Artacho ^{1,3,4}¹*Theory of Condensed Matter, Cavendish Laboratory, University of Cambridge, J. J. Thomson Ave., Cambridge CB3 0HE, United Kingdom*²*Beijing Academy of Quantum Information Sciences, Beijing 100193, China*³*CIC Nanogune BRTA and DIPC, Tolosa Hiribidea 76, 20018 San Sebastian, Spain*⁴*Ikerbasque, Basque Foundation for Science, 48011 Bilbao, Spain* (Received 31 March 2022; revised 5 August 2022; accepted 21 September 2022; published 3 November 2022)

The process by which a nuclear projectile is decelerated by the electrons of the condensed matter it traverses is currently being studied by following the explicit dynamics of projectile and electrons from first principles in a simulation box with a sample of the host matter in periodic boundary conditions. The approach has been quite successful for diverse systems even in the strong-coupling regime of maximal dissipation. This technique is here revisited for periodic solids in light of the Floquet theory of stopping, a time-periodic scattering framework characterizing the stationary dynamical solutions for a constant velocity projectile in an infinite solid. The effect of proton projectiles in diamond is studied under that light, using time-dependent density-functional theory in real time. The Floquet quasienergy-conserving stationary scattering regime, characterized by time-periodic properties such as particle density and the time derivative of energy, is obtained for a converged system size of 1000 atoms. The validity of the customary calculation of electronic stopping power from the average slope of the density-functional total energy is discussed. Quasienergy conservation, as well as the implied fundamental approximations, are critically reviewed.

DOI: [10.1103/PhysRevResearch.4.043077](https://doi.org/10.1103/PhysRevResearch.4.043077)**I. INTRODUCTION**

The quantum dynamical processes established by a swift nucleus traversing condensed matter give rise to one of the most canonical problems in nonequilibrium quantum physics. The projectile slows down when interacting with the degrees of freedom of the condensed matter host, which effectively provide a bath for what is, in effect, quite a paradigmatic quantum friction problem. In addition to its fundamental interest, the problem is of applied interest in the contexts of nuclear energy [1], space radiation [2], and medical applications such as radiation poisoning and cancer radiotherapy [3].

There are different regimes mostly depending on the charge and speed of the projectile [4,5]. For a projectile velocity $v_p \gtrsim 1$ atomic unit (1 a.u. $\approx c/137$, c being the speed of light in vacuum), the projectile energy is transferred mostly to the electrons of the host in what is called an electronic stopping process. The dissipation of projectile kinetic energy induced by a homogeneous electron liquid (jellium) offers a very appealing model system for such friction, in some sense a fermion counterpart to the Caldeira-Leggett quantum friction paradigm [6]. This theory was initially approached in the low-velocity limit [7–9], and it proved very successful in the description of the Stokes friction regime in simple metals.

It was later extended to finite velocity [10–13] or, still in the $v \rightarrow 0$ limit, to nonhomogeneous metals [14].

The importance of radiation damage in various technological contexts has given rise to a demand for estimation of electronic stopping power (S_e , the energy transfer rate from the projectile to the matter electrons) for materials beyond simple metals. This need has been addressed by Lindhard's linear response formulation for decades [15–18]. It is a general approach, allowing, in principle, for any kind of host matter, and amenable to first-principles computations [19,20]. It is, however, limited by its fundamental assumption of a weak perturbation.

Such limitation was overcome with the advent of direct numerical simulations in real time, replicating the dynamical process computationally, where a projectile is placed within a large simulation box of the host matter, normally in periodic boundary conditions, and dragged across the box at a given velocity while propagating the time-dependent Schrödinger equation in discretized real time, monitoring the electronic energy, density, and wave functions. This is done both at an empirical tight-binding level [21,22] and from first-principles using time-dependent density-functional theory (TDDFT) [23–42], achieving considerable success in the calculation of electronic stopping power for problems clearly beyond previous theoretical approaches.

Although convergence with respect to technical approximations has been thoroughly explored [43], including simulation-box finite-size convergence, the direct simulation approach rests on the assumption that the stationary regime expected for an isolated constant-velocity projectile is well approximated by the seemingly stationary situation obtained

Published by the American Physical Society under the terms of the Creative Commons Attribution 4.0 International license. Further distribution of this work must maintain attribution to the author(s) and the published article's title, journal citation, and DOI.

in the simulations. By stationary, we mean the regime in which the stopping power and deformation density (among other quantities) are time periodic as the projectile travels along a space-periodic trajectory in the host crystal.

Such stroboscopically stationary states have been the direct object of a Floquet theory of electronic stopping [44,45], which exploits the underlying discrete translational invariance in space-time for a single constant-velocity projectile moving along a space-periodic trajectory in an infinite crystal. The time-periodic deformation density and stopping power obtained from the Floquet modes should be reached in the long-time limit (always assuming constant projectile velocity). The finite periodic simulation boxes used in the direct approach cannot aim for the long-time limit, however, since after some time, the projectile reenters the already excited domain from the back or, more generally, the effect of periodic replicas of the projectile start to affect each other's dynamics, and the simulation is no longer describing what was intended. The aim is therefore for times long enough to establish a (stroboscopically) stationary single-projectile regime, but short enough that the respective perturbations associated to the each of the periodic replicas of the projectile do not have the chance to interact.

It is not known how to determine whether such a regime is reached for any particular system and velocity. Existing studies have heuristically assessed the calculations and validated the achievement of that regime by comparing with the experimentally obtained electronic stopping power. This paper aims for a better assessment and characterization of the stroboscopically stationary regime in direct simulations of bulk diamond irradiated with protons along (100), (110), and (111) high-symmetry channels, with calculations reaching up to a thousand atoms. After assessing the electronic stopping process by validating the electronic stopping power, a discussion of the Floquet theory interpretation of the results is presented, and its pertinence is validated by the obtained stationarity of the relevant quantities. Several key approximations are implied in both real-time simulations and the Floquet theory of stopping, such as classical nuclei, and a constant-velocity projectile. They are well justified in relevant physical regimes and widely used in the community, as already discussed in previous literature. Given their relevance to the topic of this paper, a critical review of the fundamental approximations is presented in the Appendix. Finally, but importantly, a justification of the customary way of obtaining S_e in real-time TDDFT simulations as the average slope of the corresponding DFT energy is presented as well in Sec. III B.

II. METHOD

Electronic excitation characteristics (electronic stopping power, particle deformation density, and related) for a proton traveling at constant velocity across bulk diamond are calculated using TDDFT [46] propagating in discretized real time [47]. The adiabatic local-density approximation (ALDA) is used for the exchange-correlation (XC) potential, by which the potential at any given time is obtained from the particle density at the time (thereby neglecting memory effects, the nonlocality of its time dependence), and it is also taken in its local-density version (LDA) as parametrized by Perdew

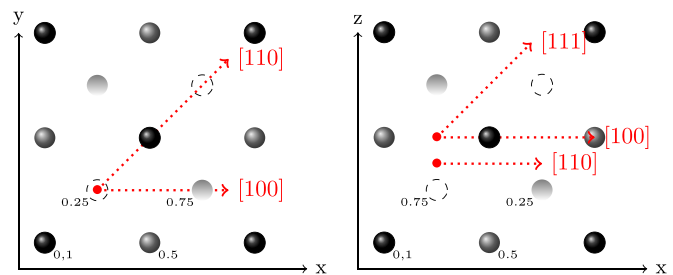


FIG. 1. (a) Diamond unit cell, looking down the [001] direction, showing the initial position of the projectile and the trajectory taken along the [100] and [110] directions. (b) Diamond unit cell, looking along the [010] direction, showing the initial heights on the projectiles along the z axis and the initial trajectories.

and Zunger [48]. Comparisons with other XC functionals have been performed for other systems elsewhere (see, e.g., Ref. [31]) and they are of no consequence to this paper.

A proton is located at an initial position within a simulation box containing a sample of the material in periodic boundary conditions. A conventional DFT calculation is first performed to obtain the initial Kohn-Sham wave functions. They are then propagated in discretized time using a Crank-Nicolson integration algorithm [47] while the proton is moved at a constant velocity through the simulation box. The electronic stopping power S_e is then obtained as the average slope of the LDA energy as the projectile moves along its trajectory [23–42]. Initial positions and trajectories used are illustrated in Fig. 1.

The TDDFT implementation [49] of the SIESTA code is used [50–53]. The publicly available open-source version of the program was used as in its master branch, commit 6c3c0249 [54]. All technical details and approximations (double- ζ or DZP basis, norm-conserving pseudopotentials) are the same as used in Ref. [42], which simulated protons through graphite. The basis set moving with the atoms (in this case, the projectile) imposes consideration of an evolving basis and Hilbert space [55]. The particulars are also as in Ref. [42]. The simulation box for the diamond sample is a $5 \times 5 \times 5$ supercell of the conventional cubic diamond cell of eight atoms, amounting to a cubic box with 1000 C atoms (plus one H projectile). The lattice parameter used was 3.567 Å.

III. RESULTS AND DISCUSSION

A. Stopping power for protons in diamond

Figures 2 and 3 show the results of the calculation of the electronic stopping power S_e for protons in diamond as a function of the projectile velocity, obtained as explained in the Method section, essentially following Refs. [23,42]. In this paper, we concentrate on velocities below the Bragg peak, a velocity range already well into the nonadiabatic regime, but still sensitive to the electronic structure of the host material (Bragg peak in the sense of the maximum in the $S_e(v)$ curve, instead of the conventional meaning of the maximum of S_e versus penetration; we will use the former meaning, henceforth). This is apparent in Fig. 2, where the calculated S_e for diamond (red squares) is compared with the results for

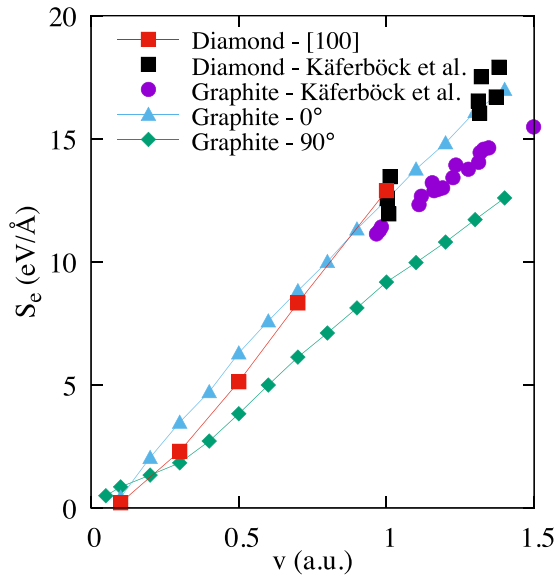


FIG. 2. Electronic stopping power S_e versus proton velocity in diamond and graphite. Simulation results for the [100] channelling trajectory in diamond (red squares) are compared with the experimental results of Ref. [56] for diamond (black squares) alongside a similar comparison for simulation results in graphite (parallel and perpendicular to graphitic planes, triangles, and rhombi, respectively) from Ref. [42], and corresponding experimental values from the same experimental paper [56] (circles).

graphite of Ref. [42] (blue and green) and both are compared with the respective experimental results of Ref. [56] (black and purple). The anisotropy in graphite gives rise to a wide band of theoretical values, already discussed in Ref. [42].

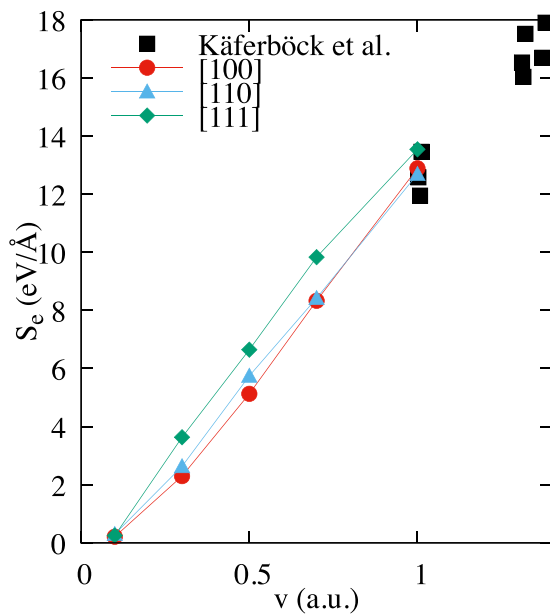


FIG. 3. Electronic stopping power S_e versus proton velocity in diamond. Simulation results for channelling trajectories along [100], [110], and [111] directions (circles, triangles, and rhombi, respectively), compared with the experimental results of Ref. [56] (squares).

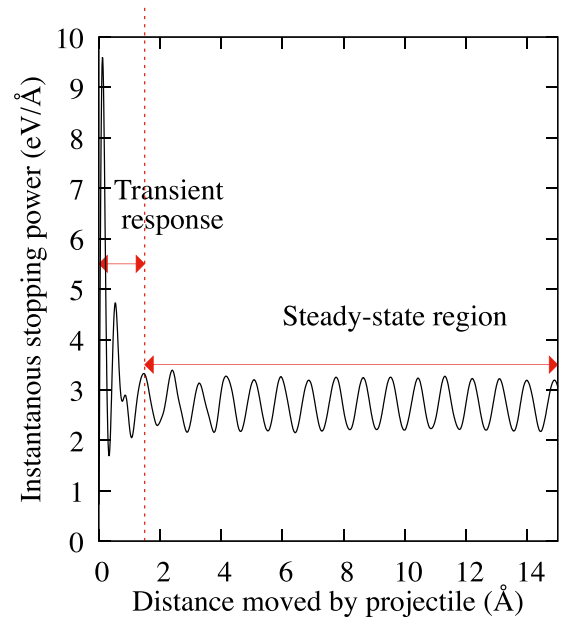


FIG. 4. Instantaneous electronic stopping power in diamond, for a proton moving through the simulation box at $v_p = 0.5$ a.u. along the [100] direction.

However, they still allow us to replicate the experimentally observed tendency toward larger stopping power for diamond for $v_p \gtrsim 1$ a.u.

Furthermore, the theoretical results display a crossover of the stopping powers where $S_e^{\text{diamond}} < S_e^{\text{graphite}}$ at lower velocities. This is a result of the threshold behavior, expected and apparent for diamond due to its large band gap. This fact cannot be validated with the available experimental data, but it does seem plausible given what is known for other large-band-gap insulators [23,57–59]. The anisotropy in S_e in diamond is less pronounced than in graphite, as shown in Fig. 3, which is again expected, in spite of the fact that the channels considered are quite different (in, e.g., electronic density). Detailed linear-response analysis on the variability of S_e for different allotropes of C and different trajectories can be found in Ref. [60]. This paper is about stationary states along channels, and what is shown in Figs. 2 and 3 is sufficient for supporting the analysis and conclusions of this paper.

The results of Figs. 2 and 3 are obtained by performing simulations at fixed v_p and obtaining the instantaneous stopping power from

$$S_e(t) = \partial_t E_{\text{ALDA}}(t)/v_p, \quad (1)$$

as displayed in Fig. 4 versus projectile position for a particular v_p value. The $S_e(t)$ profile in the figure includes an initial interval showing a transient response to the abrupt start of the projectile, which largely disappears within the first 2 Å, except for a smaller, more persistent oscillating transient. After the initial response, the steady state is quickly established. The steady-state oscillation gives a constant enough average to allow extracting the S_e values for each projectile velocity, as displayed in Figs. 2 and 3.

The range of velocities for which calculations have been performed is the one optimizing the likelihood to obtain a

good characterization of a steady state for the single-projectile problem, which is the aim of this paper. For larger velocities, the projectile traverses the cell in too short a time for the transient to disappear. We have gone up in velocity for our results to connect with experimental values, for validation, but not beyond (it represents a substantial computational effort). In the low velocity limit, the perturbation has time enough to propagate among periodic replicas, toward saturation (see Sec. III D).

B. Validity of S_e from $\partial_t E_{\text{ADFT}}$

Extracting the electronic stopping power S_e from Eq. (1), as done in the previous subsection, has been routinely done in TDDFT simulations of stopping using adiabatic forms of the exchange and correlation functional (ADFT) [23–42] since their beginning [23]. It is a sensible approach, which has been supported by agreement with experiments and by a conservation argument [61]. To our knowledge, however, it has not been more formally justified so far, which we do here.

It is indeed quite a different approach to the ones in the pre-existing literature, most prominently, the one based on scattering theory in jellium [7] and its generalizations [10–13,44]. There, S_e is given essentially by stating the energy transfer rate for each incoming state i (occupied in the laboratory frame) as

$$\partial_t E_i = n_i \sum_o (\epsilon_o - \epsilon_i) |\mathcal{S}_{i \rightarrow o}|^2 v_o \quad (2)$$

where ϵ_i and ϵ_o are the respective single-particle energies of incoming and outgoing waves in the laboratory frame, $\mathcal{S}_{i \rightarrow o}$ is the scattering amplitude for that process, v_o the outgoing group velocity, and n_i the incoming density, all now in the projectile frame. The stopping power then follows summing over all scattering processes from all the incoming occupied states to compatible unoccupied states in the laboratory frame divided by the projectile velocity for conversion, as $S_e \sim (\sum_i \partial_t E_i)/v_p$.

Although perfectly sound and valid for independent electrons, such an expression for S_e within a DFT framework relies on the relation between the total electronic energy and the single-particle Kohn-Sham eigenvalues. That connection is made through Janak's theorem [62], but, as is well known in the context of the insulator band-gap problem [63], it implies a further approximation, especially for nonmetals. This is elegantly shown in Ref. [19], where a correct expression is presented in the same vein using TDDFT in the frequency domain for the low-projectile-velocity limit in metals. A further many-electron term is there shown to appear for the correct stopping power expression for a given XC functional.

The S_e calculation in real-time TDDFT simulations as extracted from Eq. (1) is not limited to low-velocity projectiles or metals. Its justification can be seen as follows. TDDFT with the exact XC (and with proper account of the initial state) would give the exact evolving particle density $n(\mathbf{r}, t)$, in addition to the relevant action [46,64]. TDDFT also states that any physical property would be expressible as a functional of that density, although, *a priori*, the expression of that functional would not be known in general.

However, the functional for the electronic stopping power is known. It is nothing but the net force on the projectile [61,65], suitably averaged along the trajectory (and over different trajectories depending on the experimental conditions). As long as the potential V_{ext} describing the interaction between each electron and the nuclei is local, which is a prerequisite for TDDFT (and DFT in general), the instantaneous force on the projectile due to the electrons is simply

$$\mathbf{F}_p(t) = - \int d^3\mathbf{r} n(\mathbf{r}, t) \nabla_p V_{\text{ext}}, \quad (3)$$

where V_{ext} is the single-particle external potential acting on electrons due to nuclear attractions and other possible external fields. This expression is obtained very generally for Ehrenfest dynamics using Newton's law for the classical evolution of the nuclei and TDDFT for the quantum evolution of electrons [66–68]. In our case, for a classical nuclear projectile of constant velocity and other classical nuclei at rest, it is easy to corroborate, given the evolution of the electronic energy

$$\begin{aligned} \partial_t E_e &= \partial_t \langle \Psi | H | \Psi \rangle = \langle \Psi | \partial_t H | \Psi \rangle = \mathbf{v}_p \cdot \langle \Psi | \nabla_p H | \Psi \rangle \\ &= \mathbf{v}_p \cdot \int d^3\mathbf{r} n(\mathbf{r}, t) \nabla_p V_{\text{ext}} = -\mathbf{v}_p \cdot \mathbf{F}_p \end{aligned} \quad (4)$$

for any \mathbf{v}_p , and where we have used $|\Psi\rangle$ for the exact evolving electronic state and H for the electronic Hamiltonian, which fulfill $H|\Psi\rangle = i\hbar\partial_t|\Psi\rangle$, and the fact that the only explicit time dependence in the electronic Hamiltonian is given by the motion of the projectile. Therefore, a trajectory average of the force in Eq. (3) gives the electronic stopping power S_e within TDDFT and the approximations described so far. Most of the electronic stopping power evaluations in direct real-time TDDFT simulations resort to the electronic energy directly [23,61] by extracting S_e from the average slope of the electronic energy as the projectile progresses, as in Eq. (1). For the adiabatic functionals they use, the electronic energy is what is given by the corresponding time-independent density functional for the instantaneous density, in this case LDA. In that sense, $E_{\text{ADFT}} = E_{\text{LDA}}[n(\mathbf{r}, t)]$ is taken as the functional of the density for $\langle \Psi(t) | H(t) | \Psi(t) \rangle$, using the nomenclature of Eq. (4). First, it leads to the consistently correct adiabatic energy in the $v_p \rightarrow 0$ limit. Second, for any adiabatic time-dependent XC functional, the XC action can be expressed as

$$A_{\text{XC}}[n(\mathbf{r}, t)] = \int dt E_{\text{XC}}[n(\mathbf{r})](t),$$

and then the quantity

$$E_{\text{tot}} = E_{\text{ADFT}} + T_N + \sum_{I, J < I} \frac{Z_I Z_J}{R_{IJ}}$$

is shown to be conserved in Ehrenfest dynamics [66,67,69], where T_N stands for the nuclear kinetic energy. From Eq. (4), it can be seen that the calculation of S_e from the slope of the electronic energy and from the force as in Eq. (3) are equivalent. Therefore, a calculation of S_e based on Eq. (1) is well supported by TDDFT, and gives the correct value within the theory defined by the chosen XC, as long as it is an adiabatic functional. If the nonlocality in time is considered, Eq. (1) should not be used, but rather S_e should be extracted from the average force on the projectile, Eq. (3).

C. Steady state

The Floquet theory of electronic stopping [44,45] describes the stationary state for a single projectile at constant velocity the approximations and assumptions implied, such as a non-relativistic classical nuclear projectile and constant velocity, are critically reviewed in the Appendix, while size effects in the approach to an apparent stationary state are reviewed in Ref. [61]). It is a stroboscopically stationary state, meaning that properties that do not scale with the size of the system are invariant when looked at times separated by a time period $\tau = a/v_p$, where a is the lattice parameter of the one-dimensional lattice along the rectilinear projectile trajectory. The particle density $n(\mathbf{r}, t)$, the force opposing the projectile motion $\mathbf{F}_p(t)$, and, therefore, the electron energy excitation rate, $\partial_t E_e = v_p S_e$, are all stroboscopically stationary quantities, both in an exact solution and within our ALDA approach.

Since the time average of $\partial_t E_e$ is not zero, the electronic energy itself steadily grows, and it is therefore not a stroboscopically stationary property. This is compatible with Floquet theorem since it is an infinite open system. It is analogous to a scattering problem in general, and to the stopping problem in jellium, in particular, which is time independent, with constant S_e and therefore increasing E_e . There are properties relating to the Kohn-Sham single-particle states that are also stroboscopically stationary [70], but we concentrate here on energy, density, and forces.

Figure 4 clearly displays the described expectation for $\partial_t E_e$: after the transient, an oscillatory behavior for, in this case, the time derivative of the electronic energy, with the expected period (the lattice parameter along [100] is $a = 3.567 \text{ \AA}$, the projectile passing close to a C atom every $a/4 = 0.89 \text{ \AA}$, which perfectly conforms with the observed periodicity). Figure 5 shows the repetition of the dynamical deformation density at equivalent proton positions (and corresponding times) in the diamond crystal, for the projectile moving at $v_p = 1 \text{ a.u.}$ along the [110] direction. The dynamical deformation density is defined as

$$\delta n^{\text{dyn}}(\mathbf{r}, t) = n(\mathbf{r}, t) - n^a[\mathbf{r}, \{\mathbf{R}_I(t)\}];$$

$n(\mathbf{r}, t)$ being the dynamical electron density and $n^a[\mathbf{r}, \{\mathbf{R}_I(t)\}]$ the corresponding adiabatic electron density, meaning the one corresponding to the electronic ground state for the nuclei at their \mathbf{R}_I positions at time t .

There are depictions in the literature of the wake of the projectile in terms of maps of the density or the deformation density (see, e.g., very early sets in Refs. [71,72] for jellium, and also for metals such as on the cover of the issue for Ref. [27] and in Refs. [36,61], for example). A comparative wake analysis for different velocities, directions, and materials would be of interest. It is, however, beyond the scope of this paper; our focus is on the stroboscopic stationarity of the density as key magnitude in first-principles calculations of these processes. The key comparison is therefore between the upper and lower panels of Fig. 5. Indeed, the deformation density pattern is very rich and intricate, and the similarity under translation is remarkable.

For a more quantitative assessment, Fig. 6 shows the same deformation density along the projectile path at different

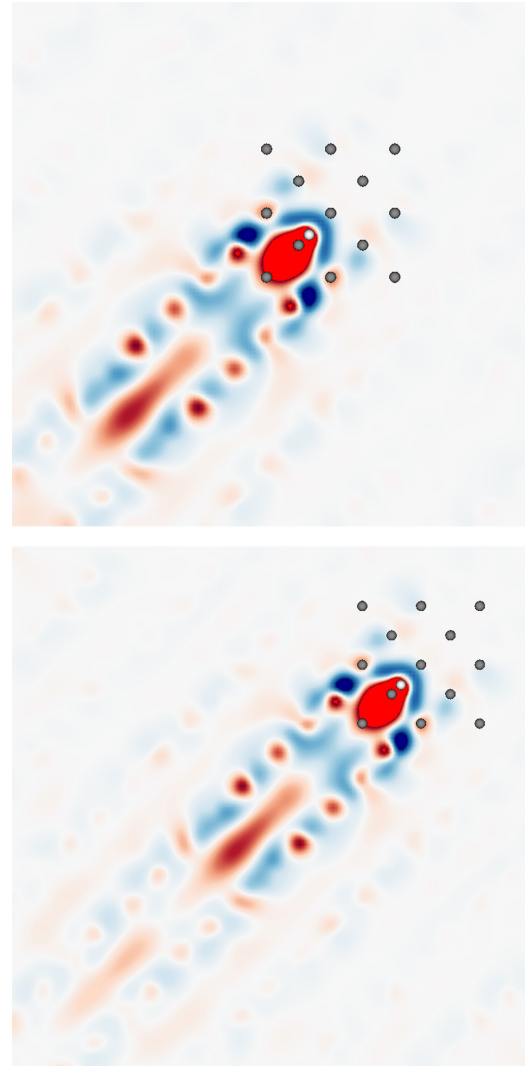


FIG. 5. Electron deformation density in real space at equivalent projectile positions in consecutive diamond unit cells (upper and lower panels) along the trajectory for a proton moving at $v = 1 \text{ a.u.}$ along the [110] direction. It is depicted in the (001) plane containing the projectile, the horizontal axis being the [100] direction and the vertical axis the [010] direction. The color scale is given from -0.01 e/Bohr (dark blue) to $+0.01 \text{ e/Bohr}$ (dark red), going through white for zero. The homogeneous bright red close to the proton is saturated (scale chosen to show rich pattern in the tail). Beads indicate atomic positions of selected atoms including the projectile (light bead) to indicate the equivalence of position under translation.

projectile positions that are crystallographically equivalent, taking the projectile position as a reference for better comparison. It is shown for low (0.1 a.u.) and high (1.0 a.u.) velocity. It can be seen how the deformation tends to stabilize in the latter positions, once the projectile has approached the stationary state. It can be appreciated that the stationarity is only approximate, with small differences between the last two points, points 4 and 5 (spiky features in the lower panel relate to the real-space discretization inherent to the SIESTA method [52]).

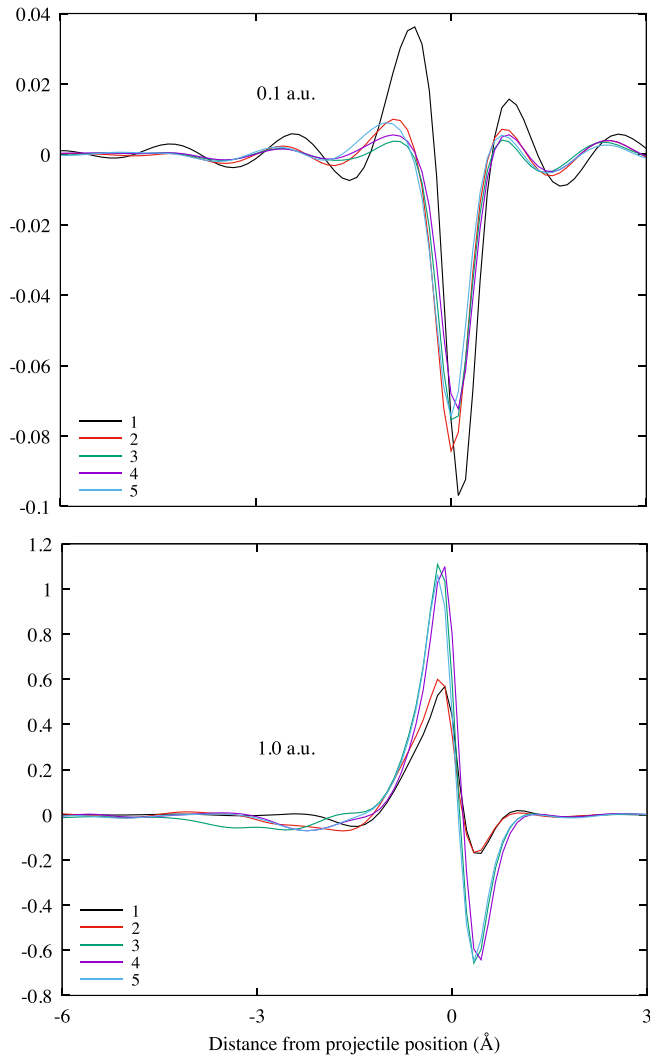


FIG. 6. Electron deformation density along the path of the projectile, comparing for projectile positions at five different points in the simulation box which are crystallographically equivalent, labeled 1–5, the number increasing the more advanced the projectile. Upper (lower) panel is for $v_p = 0.1$ a.u. (1.0 a.u.).

D. Saturation

For the single-projectile problem, the Floquet stationary solutions would be reached in the long-time limit (if at all). It should be noted, however, that in the periodically repeated projectile simulations described in Secs. II and III A, in the long-time limit, a different regime is to be expected. It is also a periodic problem, but one in which, due to its effective finite size (or finite host size per projectile), Floquet modes would be expected for which the electronic energy itself (not its flux) would be periodic and, therefore, the oscillating $S_e(t)$ would average to zero. Physically, since projectile replicas pump energy into the host electronic system everywhere, the system should reach a saturated periodic state, as described for finite Floquet systems (see, for instance, Refs. [73,74]), in which energy would be transferred back and forth between the projectile lattice and the electrons. It is not a regime of interest to the single-projectile problem, but can rather be considered as a finite-size effect, and the simulation box size is normally

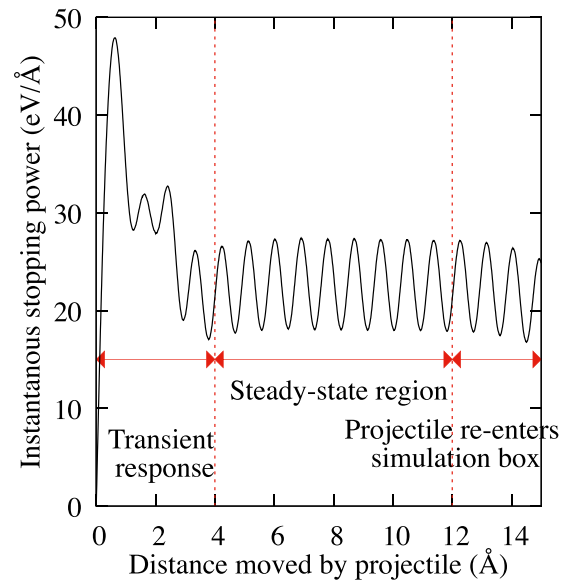


FIG. 7. Instantaneous electronic stopping power in diamond for a proton moving at $v_p = 0.1$ a.u. along the [100] direction.

increased when hints of saturation appear before a meaningful description of the intended phenomena is reached. Saturation will not be characterized here, beyond illustrating its onset in Fig. 7.

The calculation of S_e and characterization of processes of electronic stopping of projectiles by means of direct computation in a finite simulation box relies on the system reaching a regime in which the effect of other projectile replicas is still not felt by a given projectile (finding a fresh host as it moves). Each replica hence approximately behaves as a single projectile and, therefore, could achieve the stationary regime predicted by the Floquet theory of stopping [44] before the effect of other projectiles is felt (e.g., by reentering the cell, or energy irradiation from other replicas reaching the one being followed).

The sweet spot is therefore in the interval between the end of the initial transient and the onset of saturation, as illustrated in Fig. 7. It is so far hard to foretell the duration, and even the existence, of such a regime. It will depend on the projectile velocity and kind of host, as well as the type of start (smooth versus instantaneous). So far, it is addressed as a technical system-size convergence problem (see a discussion on this in Ref. [34]) and, so far, this community has been fortunate in finding most situations amenable to feasible computation.

A more fundamental problem, however, is, once a stable oscillation is found, to ascertain whether what observed really corresponds to the actually sought Floquet stationary regime of the stopping problem. The thermalization of such a system into the steady nonequilibrium regime does not appear to be a trivial problem. Some correlated systems are known not to thermalize to equilibrium while stuck in a many-body localized state [75–77]. In the strongly out-of-equilibrium problem presented by electronic stopping in various kinds of solids, we are not aware of any way of ascertaining on reaching the relevant steady state. Helpful here would be the calculation of the Floquet stationary state directly on a TDDFT implementation

of the scattering Floquet theory of stopping, analogous to what accomplished in Ref. [45] for a tight-binding Hamiltonian. That should be the focus of further work.

IV. CONCLUSIONS

Based on results for the electronic stopping power for protons in diamond, the results of such simulations are analyzed in light of the stroboscopic stationary states predicted by the recent Floquet theory of stopping. The predicted Floquet solutions for the electronic excitation by a projectile are distinguished from the ones expected for a lattice of projectiles, the latter corresponding to the actual supercell calculations, the former to the physical process of interest.

The intermediate regime between the initial transient behavior due to the start of the projectile motion and the onset of saturation is shown to reflect the stroboscopic stationary state of the single projectile, and the stationary character is tested quantitatively. The results for S_e and particle density for protons in diamond display remarkable stroboscopic invariance of both magnitudes in that regime.

The average of $\partial_t E_e/v_p$ is shown to give the correct electronic stopping power S_e , within TDDFT, supporting the way it has been calculated in many electronic stopping studies, but only for adiabatic time-dependent XC functionals. For density functionals beyond that approximation (contemplating the nonlocality of the time dependence), the force on the projectile should be used instead.

ACKNOWLEDGMENTS

We are grateful to N. Koval and D. Muñoz-Santiburcio for their help with securing and managing the computational resources needed for this project. J.F.K.H. would like to acknowledge the EPSRC Centre for Doctoral Training in Computational Methods for Materials Science for funding under Grant No. EP/L015552/1. E.A. and M.F. acknowledge funding from the Leverhulme Trust, under Research Project Grant No. RPG-2018-254, E.A. is grateful for funding from the EU through the ElectronStopping Grant No. 333813, within the Marie-Sklodowska-Curie CIG program, and by the Research Executive Agency under the European Union's Horizon 2020 Research and Innovation program (Project No. ESC2RAD, Grant Agreement No. 776410). Funding from Spanish MINECO is also acknowledged through Grant No. FIS2015-64886-C5-1-P and from Spanish MICIN through Grant No. PID2019-107338RB-C61/AEI/10.13039/501100011033, as well as a María de Maeztu award to Nanogune, Grant No. CEX2020-001038-M funded by MCIN/AEI/10.13039/501100011033. Computational time from CCSD3, the Cambridge Tier-2 system operated by the University of Cambridge Research Computing Service funded by the Engineering and Physical Sciences Research Council Tier-2 (capital Grant No. EP/P020259/1), and DiRAC funding from the Science and Technology Facilities Council. We also acknowledge the Partnership for Advanced Computing in Europe, PRACE, for awarding us access to computational resources in Joliot-Curie at GENCI@CEA, France, under EU-H2020 Grant No. 2019215186.

APPENDIX: REVIEW OF FUNDAMENTAL APPROXIMATIONS

The technical approximations for the direct simulation of electronic stopping processes have been studied before [43]. Here we review the more fundamental ones underlying the mentioned studies and this one. As mentioned, they follow the electronic dynamics under the time-dependent external potential originated by the nuclei of both the static host atoms and the mobile projectile. It is done for a finite box in periodic boundary conditions. As such, it is a well-defined time-dependent quantum problem for the electrons, but its relevance for the real problem relies on several basic approximations and assumptions, as follows.

1. Nonrelativistic quantum mechanics

The described simulations are based on nonrelativistic quantum mechanics, except for relativistic corrections possibly included in the pseudopotentials when containing high-velocity core electrons. A relativistic treatment of stopping is known to be needed in the high velocity regime, well beyond the Bragg peak [4], but the calculations discussed here are normally done for projectile velocities up to and around the Bragg peak. For light projectiles, the Bragg peak is around 2 a.u. of velocity. Considering that the velocity of an electron out of a collision with the projectile would be $v_e \lesssim 2v_p$ (equality for a classical head-on collision with a heavy projectile), taking $v_e = 4$ a.u., gives a kinetic energy of $T = 217.6$ eV (with a relativistic correction $\Delta T = T_{\text{rel}} - T_{\text{nr}} = 140$ meV). That kinetic energy is smaller than the one of a $2p$ electron in an aluminium atom (~ 270 eV), for which relativistic corrections are well-known to be quite unnecessary for most practical purposes of electronic structure.

The assumption should be taken with care for high-charge projectiles, however. The Bragg peak goes up to and beyond $v_p \sim 10$ a.u., and an electron with $v_e \sim 20$ a.u. has a kinetic energy of $T \sim 5.5$ keV (with $\Delta T \sim 90$ eV), comparable to much deeper core states for which relativistic corrections are known to be significant. Core states, especially of the projectile, are known to deform significantly in the stopping process, away from the free atom reference [41], implying that explicitly relativistic calculations could be needed when facing the dynamical problem including those core electrons. It should be kept in mind that in those cases, the core electrons significantly perturb from their usual atomic state, rendering many all-electron approaches, such as the augmented plane-wave [78] or projector augmented-wave [79] methods, not suitable for the problem, which demands flexible, nonspherical treatment of the relativistic Dirac problem.

2. Classical nuclei

The approach assumes classical nuclei, which, together with the quantum electrons define Ehrenfest dynamics. It is known that beyond-Ehrenfest approaches are needed for the correct long-time thermalization of the excess energy accumulated in the host [68,80–82]. Essentially, the spontaneous emission of phonons is a thermalization channel that is closed if the quantum fluctuations of nuclear motion are not included. They are much less important for the electronic

energy uptake from the projectile motion in the short timescale [83,84], which is the focus of this and similar electronic stopping studies. Simulating beyond Ehrenfest, including quantum fluctuations for the nuclear motion, is doable, although considerably more costly computationally. The most popular approaches are based on the surface-hopping method and variants thereof [85,86], but they are generally and better devised for finite systems with well-separated potential energy surfaces, unlike the continuum of excitations encountered in the electronic stopping problem. More suitable would be the coupled-electron-ion dynamics approach of Ref. [80], and the many-trajectory sampling with Bohmian dynamics of Refs. [87,88], although the computational effort is hugely increased. Recent progress in exact factorization techniques [81,89] also offers interesting possibilities. To our knowledge, a quantitative assessment of such effects in electronic stopping is still lacking.

3. Constant projectile velocity

In most electronic stopping theory and simulation studies, the projectile is taken to travel at constant velocity. It is quite a tradition in the field due to the fact, on one hand, that it is inherent to prevalent theories, both in linear response [15,20] and in the nonlinear theory based on a Galilean transformation to the constant-velocity reference frame sitting on the projectile [7,9,44]. On the other hand, it is also handy for its applicability in radiation damage, where the velocity-dependence of the electronic stopping power is very generally used. It is, of course, an approximation (see a general assessment in Ref. [61]), the projectile slowing down with a net deceleration of magnitude $a = S_e/m_p$. The maximum deceleration would happen for velocities around the Bragg peak. With $S_e \sim 13 \text{ eV/\AA}$, for example, for protons in diamond, it amounts to $a = 1.4 \times 10^{-4} \text{ a.u.}$ Across the 33.7 Bohr simulation box in the calculations described above, within which the steady stopping regime seems to be well established, an initial velocity of 2 a.u. would diminish by $4.7 \times 10^{-3} \text{ a.u.}$, or 0.24%. Similarly, trajectory deflection is negligible except for very small impact parameters. This consideration connects with the trajectory sampling problem, which has been discussed at length (see, e.g., Ref. [61] and references therein), including studies with full Ehrenfest dynamics, which allow for slowing down and deflection of the projectile. For the purposes of this paper, however, a constant velocity along high-symmetry channels is considered, as it is a problem that is particularly suited for the intended analysis.

4. Electron exchange and correlation

The electron-electron interaction and correlation in direct electronic stopping simulations is normally considered [61] within TDDFT [46,64], which is, in principle, exact, except for the approximate XC potentials used. So far, and to our knowledge, potentials without history dependence have been used (local in time), assuming locality in space as well (LDA) or generalized gradient approximations, such as that in Ref. [90]. History dependence is included in Ref. [19] via linear-response TDDFT in the low-velocity regime. There is quite

a scope for improvement on this front, both in the space and time dependencies of the XC potential, although work so far, including validation with experiments, does not point to XC errors as prominent, within the kind of simulations studied here. The approximation is discussed in some depth for the electronic stopping problem in Refs. [39,91]. The work in Refs. [14,19] point in the direction of time-dependent current density functional theory as a very promising route to capture the nonlocalities of space and time in a much more physically meaningful manner. Here we still use the ALDA approximation and focus on other issues.

5. Conservation

Here it is important to clarify some notions on energy conservation. Starting from the obvious, the dynamics of the projectile itself is dissipative under the friction provided by the degrees of freedom of the host, while the dynamics of the whole projectile plus host electrons and nuclei conserves the total energy. As mentioned above, the latter conservation is kept within Ehrenfest dynamics, with quantum electrons and classical nuclei. Also obviously, the constant-projectile-velocity problem is not conservative, the constraining force acting on the projectile to keep its constant velocity generating a work that increases the energy of the host.

A change of reference frame modifies the energetics. For the particular case of a jellium host, a change of reference frame was central to the jellium nonlinear theory of electronic stopping [7]. It was changed from the reference in which the electron liquid is at rest (equilibrium, the laboratory frame) to the one sitting on the projectile. The Galilean boost transforms the problem of a projectile through an homogeneous electron liquid in equilibrium into that of an impurity in the homogeneous electron liquid sustaining a current equal to $-nv_p e$, where e is the charge of the electron and n is the constant particle density of the liquid. Again the system can be seen as conservative when following the dynamics of all particles, but also as dissipative inasmuch the electron scattering off the impurity transforms part of the energy associated to the current into heat.

It is important to distinguish the above discussion from what happens in each one of the single-particle scattering events or the scattering of each of the auxiliary fermions in the Kohn-Sham problem in DFT. Still, in the jellium case, each one of those processes is conservative in the projectile reference frame: a quantum particle scattering off the static external potential defined by the impurity. Indeed, the problem has become time independent and it is the time-independent Schrödinger equation (or Kohn-Sham) being solved.

When changing to the laboratory frame, however, energy is transferred in each event from the moving projectile scatterer to the scattered electron, making it nonconservative. This consideration is what gives rise to the stopping power obtained as derived from Eq. (2). The same discussion is generalized beyond jellium to a constant velocity projectile moving along a periodic trajectory in a crystalline solid. The Kohn-Sham scattering events conserve Floquet quasienergy in the projectile reference frame [44], and a Galilean boost to the laboratory frame breaks that conservation, in perfect analogy to (generalization of) the jellium case.

- [1] R. E. Nightingale, *Nuclear Graphite* (Academic Press, London and New York, 1962).
- [2] M. Bagatin and S. Gerardin, *Ionizing Radiation Effects in Electronics: From Memories to Imagers*, (CRC Press, Taylor and Francis, Boca Raton, FL, 2016).
- [3] W. P. Levin, H. Kooy, J. S. Loeffler, and T. F. DeLaney, Proton beam therapy, *British J. Cancer* **93**, 849 (2005).
- [4] P. Sigmund, *Particle Penetration and Radiation Effects* (Springer International Publishing, Berlin, 2006).
- [5] P. Sigmund, *Particle Penetration and Radiation Effects* (Springer International Publishing, Berlin, 2014), Vol. 2.
- [6] A. O. Caldeira and A. J. Leggett, Influence of Dissipation on Quantum Tunneling in Macroscopic Systems, *Phys. Rev. Lett.* **46**, 211 (1981).
- [7] P. Echenique, R. Nieminen, and R. Ritchie, Density functional calculation of stopping power of an electron gas for slow ions, *Solid State Commun.* **37**, 779 (1981).
- [8] P. M. Echenique, R. M. Nieminen, J. C. Ashley, and R. H. Ritchie, Nonlinear stopping power of an electron gas for slow ions, *Phys. Rev. A* **33**, 897 (1986).
- [9] P. M. Echenique, F. Flores, and R. H. Ritchie, *Dynamic Screening of Ions in Condensed Matter*, Solid State Physics Series, Vol. 43, edited by H. Ehrenreich and D. Turnbull (Academic Press, New York, 1990), pp. 229–308.
- [10] K. Schönhammer, Nonlinear friction in a homogenous electron gas: Exact results, *Phys. Rev. B* **37**, 7735 (1988).
- [11] L. Bönig and K. Schönhammer, Time-dependent local perturbation in a free-electron gas: Exact results, *Phys. Rev. B* **39**, 7413 (1989).
- [12] E. Zaremba, A. Arnau, and P. Echenique, Nonlinear screening and stopping powers at finite projectile velocities, *Nucl. Instrum. Methods B* **96**, 619 (1995).
- [13] A. F. Lifschitz and N. R. Arista, Velocity-dependent screening in metals, *Phys. Rev. A* **57**, 200 (1998).
- [14] V. Nazarov, J. Pitarke, Y. Takada, G. Vignale, and Y.-C. Chang, Including nonlocality in the exchange-correlation kernel from time-dependent current density functional theory: Application to the stopping power of electron liquids, *Phys. Rev. B* **76**, 205103 (2007).
- [15] J. Lindhard, On the properties of a gas of charged particles, *Mat. Fys. Medd. K. Dan. Vidensk. Selsk.* **28**, 1 (1954).
- [16] J. Lindhard and M. Scharff, Energy dissipation by ions in the kev region, *Phys. Rev.* **124**, 128 (1961).
- [17] J. Lindhard, M. Scharff, and H. E. Schiött, Range concepts and heavy ion ranges, *Mat. Fys. Medd. K. Dan. Vidensk. Selsk.* **33**, 1 (1963).
- [18] J. Lindhard, Influence of crystal lattice on motion of energetic charged particles, *Mat. Fys. Medd.* **34**, 1 (1965).
- [19] V. U. Nazarov, J. M. Pitarke, C. S. Kim, and Y. Takada, Time-dependent density-functional theory for the stopping power of an interacting electron gas for slow ions, *Phys. Rev. B* **71**, 121106(R) (2005).
- [20] A. A. Shukri, F. Bruneval, and L. Reining, Ab initio electronic stopping power of protons in bulk materials, *Phys. Rev. B* **93**, 035128 (2016).
- [21] D. R. Mason, J. le Page, C. P. Race, W. M. C. Foulkes, M. W. Finnis, and A. P. Sutton, Electronic damping of atomic dynamics in irradiation damage of metals, *J. Phys.: Condens. Matter* **19**, 436209 (2007).
- [22] C. P. Race, D. R. Mason, M. W. Finnis, W. M. C. Foulkes, A. P. Horsfield, and A. P. Sutton, The treatment of electronic excitations in atomistic models of radiation damage in metals, *Rep. Prog. Phys.* **73**, 116501 (2010).
- [23] J. M. Pruneda, D. Sánchez-Portal, A. Arnau, J. I. Juaristi, and E. Artacho, Electronic Stopping Power in LiF from First Principles, *Phys. Rev. Lett.* **99**, 235501 (2007).
- [24] A. V. Krasheninnikov, Y. Miyamoto, and D. Tománek, Role of Electronic Excitations in Ion Collisions with Carbon Nanostructures, *Phys. Rev. Lett.* **99**, 016104 (2007).
- [25] M. Quijada, A. G. Borisov, I. Nagy, R. D. Muñio, and P. M. Echenique, Time-dependent density-functional calculation of the stopping power for protons and antiprotons in metals, *Phys. Rev. A* **75**, 042902 (2007).
- [26] R. Hatcher, M. Beck, A. Tackett, and S. T. Pantelides, Dynamical Effects in the Interaction of Ion Beams with Solids, *Phys. Rev. Lett.* **100**, 103201 (2008).
- [27] A. A. Correa, J. Kohanoff, E. Artacho, D. Sánchez-Portal, and A. Caro, Nonadiabatic Forces in Ion-Solid Interactions: The Initial Stages of Radiation Damage, *Phys. Rev. Lett.* **108**, 213201 (2012).
- [28] M. A. Zeb, J. Kohanoff, D. Sánchez-Portal, A. Arnau, J. I. Juaristi, and E. Artacho, Electronic Stopping Power in Gold: The Role of d Electrons and the H/He Anomaly, *Phys. Rev. Lett.* **108**, 225504 (2012).
- [29] M. A. Zeb, J. Kohanoff, D. Sánchez-Portal, and E. Artacho, Electronic stopping power of H and He in Al and LiF from first principles, *Nucl. Instrum. Methods B* **303**, 59 (2013).
- [30] A. Ojanperä, A. V. Krasheninnikov, and M. Puska, Electronic stopping power from first-principles calculations with account for core electron excitations and projectile ionization, *Phys. Rev. B* **89**, 035120 (2014).
- [31] R. Ullah, F. Corsetti, D. Sánchez-Portal, and E. Artacho, Electronic stopping power in a narrow band gap semiconductor from first principles, *Phys. Rev. B* **91**, 125203 (2015).
- [32] W. Li, X. Wang, X. Zhang, S. Zhao, H. Duan, and J. Xue, Mechanism of the defect formation in supported graphene by energetic heavy ion irradiation: The substrate effect, *Sci. Rep.* **5**, 9935 (2015).
- [33] Z. Wang, S.-S. Li, and L.-W. Wang, Efficient Real-Time Time-Dependent Density Functional Theory Method and Its Application to a Collision of an Ion with a 2D Material, *Phys. Rev. Lett.* **114**, 063004 (2015).
- [34] A. Schleife, Y. Kanai, and A. A. Correa, Accurate atomistic first-principles calculations of electronic stopping, *Phys. Rev. B* **91**, 014306 (2015).
- [35] A. Lim, W. M. C. Foulkes, A. P. Horsfield, D. R. Mason, A. Schleife, E. W. Draeger, and A. A. Correa, Electron Elevator: Excitations Across the Band Gap via a Dynamical Gap State, *Phys. Rev. Lett.* **116**, 043201 (2016).
- [36] E. E. Quashie, B. C. Saha, and A. A. Correa, Electronic band structure effects in the stopping of protons in copper, *Phys. Rev. B* **94**, 155403 (2016).
- [37] K. G. Reeves, Y. Yao, and Y. Kanai, Electronic stopping power in liquid water for protons and α particles from first principles, *Phys. Rev. B* **94**, 041108(R) (2016).
- [38] C.-K. Li, F. Wang, B. Liao, X.-P. OuYang, and F.-S. Zhang, Ab initio electronic stopping power and threshold effect of channeled slow light ions in HfO₂, *Phys. Rev. B* **96**, 094301 (2017).

- [39] D. C. Yost, Y. Yao, and Y. Kanai, First-principles modeling of electronic stopping in complex matter under ion irradiation, *J. Phys. Chem. Lett.* **11**, 229 (2019).
- [40] G. Bi, J. Kang, and L.-W. Wang, High velocity proton collision with liquid lithium: A time dependent density functional theory study, *Phys. Chem. Chem. Phys.* **19**, 9053 (2017).
- [41] R. Ullah, E. Artacho, and A. A. Correa, Core Electrons in the Electronic Stopping of Heavy Ions, *Phys. Rev. Lett.* **121**, 116401 (2018).
- [42] J. Halliday and E. Artacho, Anisotropy of electronic stopping power in graphite, *Phys. Rev. B* **100**, 104112 (2019).
- [43] D. C. Yost, Y. Yao, and Y. Kanai, Examining real-time time-dependent density functional theory nonequilibrium simulations for the calculation of electronic stopping power, *Phys. Rev. B* **96**, 115134 (2017).
- [44] N. Forcellini and E. Artacho, Floquet theory for the electronic stopping of projectiles in solids, *Phys. Rev. Res.* **2**, 033151 (2020).
- [45] M. Famili, N. Forcellini, and E. Artacho, Local orbital formulation of the Floquet theory of projectile electronic stopping, *Phys. Rev. B* **105**, 245139 (2022).
- [46] M. Marques, A. Rubio, E. K. Gross, K. Burke, F. Nogueira, and C. A. Ullrich, *Time-dependent Density Functional Theory*, Lecture Notes in Physics, Springer Science & Business Media (Springer, Berlin, 2006).
- [47] A. Tsolakidis, D. Sánchez-Portal, and R. M. Martin, Calculation of the optical response of atomic clusters using time-dependent density functional theory and local orbitals, *Phys. Rev. B* **66**, 235416 (2002).
- [48] J. P. Perdew and A. Zunger, Self-interaction correction to density-functional approximations for many-electron systems, *Phys. Rev. B* **23**, 5048 (1981).
- [49] A. García, N. Papior, A. Akhtar, E. Artacho, V. Blum, E. Bosoni, P. Brandimarte, M. Brandbyge, J. I. Cerdá, F. Corsetti *et al.*, Siesta: Recent developments and applications, *J. Chem. Phys.* **152**, 204108 (2020).
- [50] P. Ordejón, E. Artacho, and J. M. Soler, Self-consistent order-n density-functional calculations for very large systems, *Phys. Rev. B* **53**, R10441 (1996).
- [51] E. Artacho, D. Sánchez-Portal, P. Ordejón, A. Garcia, and J. M. Soler, Linear-scaling ab-initio calculations for large and complex systems, *Phys. Status Solidi B* **215**, 809 (1999).
- [52] J. M. Soler, E. Artacho, J. D. Gale, A. García, J. Junquera, P. Ordejón, and D. Sánchez-Portal, The SIESTA method for ab initio order-N materials simulation, *J. Phys.: Condens. Matter* **14**, 2745 (2002).
- [53] E. Artacho, E. Anglada, O. Dieguez, J. D. Gale, A. Garcia, J. Junquera, R. M. Martin, P. Ordejon, J. M. Pruneda, D. Sanchez-Portal, and J. M. Soler, The SIESTA method; developments and applicability, *J. Phys.: Condens. Matter* **20**, 064208 (2008).
- [54] COMMIT 6C3C0249, <https://gitlab.com/siesta-project> (accessed Jan. 29, 2021)
- [55] E. Artacho and D. D. O'Regan, Quantum mechanics in an evolving Hilbert space, *Phys. Rev. B* **95**, 115155 (2017).
- [56] W. Käferböck, W. Rössler, V. Necas, P. Bauer, M. Peñalba, E. Zarate, and A. Arnau, Comparative study of the stopping power of graphite and diamond, *Phys. Rev. B* **55**, 13275 (1997).
- [57] M. Draxler, S. Chenakin, S. Markin, and P. Bauer, Apparent Velocity Threshold in the Electronic Stopping of Slow Hydrogen Ions in LiF, *Phys. Rev. Lett.* **95**, 113201 (2005).
- [58] S. Markin, D. Primetzhofer, and P. Bauer, Vanishing Electronic Energy Loss of Very Slow Light Ions in Insulators with Large Band Gaps, *Phys. Rev. Lett.* **103**, 113201 (2009).
- [59] D. Roth, B. Bruckner, G. Undeutsch, V. Paneta, A. I. Mardare, C. L. McGahan, M. Dosmailov, J. I. Juaristi, M. Alducin, J. D. Pedarnig, R. F. Haglund, D. Primetzhofer, and P. Bauer, Electronic Stopping of Slow Protons in Oxides: Scaling Properties, *Phys. Rev. Lett.* **119**, 163401 (2017).
- [60] R. Garcia-Molina, I. Abril, C. D. Denton, and S. Heredia-Avalos, Allotropic effects on the energy loss of swift H⁺ and He⁺ ion beams through thin foils, *Nucl. Instrum. Methods B* **249**, 6 (2006).
- [61] A. A. Correa, Calculating electronic stopping power in materials from first principles, *Comput. Mater. Sci.* **150**, 291 (2018).
- [62] J. F. Janak, Proof that $\partial E/\partial n_i = \varepsilon_i$ in density-functional theory, *Phys. Rev. B* **18**, 7165 (1978).
- [63] L. J. Sham and M. Schlüter, Density-Functional Theory of the Energy Gap, *Phys. Rev. Lett.* **51**, 1888 (1983).
- [64] E. Runge and E. K. U. Gross, Density-Functional Theory for Time-Dependent Systems, *Phys. Rev. Lett.* **52**, 997 (1984).
- [65] P. L. Grande, Alternative treatment for the energy-transfer and transport cross section in dressed electron-ion binary collisions, *Phys. Rev. A* **94**, 042704 (2016).
- [66] U. Saalmann and R. Schmidt, Non-adiabatic quantum molecular dynamics: Basic formalism and case study, *Z. Phys. D* **38**, 153 (1996).
- [67] T. Todorov, Time-dependent tight binding, *J. Phys.: Condens. Matter* **13**, 10125 (2001).
- [68] B. F. Curchod, U. Rothlisberger, and I. Tavernelli, Trajectory-based nonadiabatic dynamics with time-dependent density functional theory, *Chem. Phys. Chem.* **14**, 1314 (2013).
- [69] T. Kunert and R. Schmidt, Non-adiabatic quantum molecular dynamics: General formalism and case study H₂⁺ in strong laser fields, *Eur. Phys. J. D* **25**, 15 (2003).
- [70] See, e.g., the spectral projections presented in Ref. [28]. Scattering amplitudes can be defined for the single-particle scattering processes in the projectile reference frame and within the Floquet theory [44,45]. Matrix elements that make sense for supercell time-dependent simulations may, however, steadily increase with time due to the flux implied in scattering (see Fig. 2 in Ref. [28]).
- [71] R. Ritchie, W. Brandt, and P. Echenique, Wake potential of swift ions in solids, *Phys. Rev. B* **14**, 4808 (1976).
- [72] P. Echenique, R. Ritchie, and W. Brandt, Spatial excitation patterns induced by swift ions in condensed matter, *Phys. Rev. B* **20**, 2567 (1979).
- [73] L. D'Alessio and M. Rigol, Long-Time Behavior of Isolated Periodically Driven Interacting Lattice Systems, *Phys. Rev. X* **4**, 041048 (2014).
- [74] A. Lazarides, A. Das, and R. Moessner, Equilibrium states of generic quantum systems subject to periodic driving, *Phys. Rev. E* **90**, 012110 (2014).
- [75] D. A. Abanin, E. Altman, I. Bloch, and M. Serbyn, Colloquium: Many-body localization, thermalization, and entanglement, *Rev. Mod. Phys.* **91**, 021001 (2019).

- [76] P. Ponte, Z. Papić, F. Huveneers, and D. A. Abanin, Many-Body Localization in Periodically Driven Systems, *Phys. Rev. Lett.* **114**, 140401 (2015).
- [77] A. Lazarides, A. Das, and R. Moessner, Fate of Many-Body Localization Under Periodic Driving, *Phys. Rev. Lett.* **115**, 030402 (2015).
- [78] G. K. Madsen, P. Blaha, K. Schwarz, E. Sjöstedt, and L. Nordström, Efficient linearization of the augmented plane-wave method, *Phys. Rev. B* **64**, 195134 (2001).
- [79] P. E. Blöchl, Projector augmented-wave method, *Phys. Rev. B* **50**, 17953 (1994).
- [80] E. J. McEniry, Y. Wang, D. Dundas, T. N. Todorov, L. Stella, R. Miranda, A. Fisher, A. Horsfield, C. Race, D. Mason *et al.*, Modelling non-adiabatic processes using correlated electron dynamics, *Eur. Phys. J. B* **77**, 305 (2010).
- [81] A. Abedi, N. T. Maitra, and E. Gross, Correlated electron-nuclear dynamics: Exact factorization of the molecular wavefunction, *J. Chem. Phys.* **137**, 22A530 (2012).
- [82] N. I. Gidopoulos and E. Gross, Electronic non-adiabatic states: Towards a density functional theory beyond the Born–Oppenheimer approximation, *Philos. Trans. R. Soc. A* **372**, 20130059 (2014).
- [83] M. Caro, A. A. Correa, E. Artacho, and A. Caro, Stopping power beyond the adiabatic approximation, *Sci. Rep.* **7**, 2618 (2017).
- [84] M. Caro, A. Tamm, A. Correa, and A. Caro, Role of electrons in collision cascades in solids. I. Dissipative model, *Phys. Rev. B* **99**, 174301 (2019).
- [85] D. S. Sholl and J. C. Tully, A generalized surface hopping method, *J. Chem. Phys.* **109**, 7702 (1998).
- [86] J. E. Subotnik, A. Jain, B. Landry, A. Petit, W. Ouyang, and N. Bellonzi, Understanding the surface hopping view of electronic transitions and decoherence, *Annu. Rev. Phys. Chem.* **67**, 387 (2016).
- [87] B. F. Curchod and I. Tavernelli, On trajectory-based nonadiabatic dynamics: Bohmian dynamics versus trajectory surface hopping, *J. Chem. Phys.* **138**, 184112 (2013).
- [88] G. Albareda and I. Tavernelli, Bohmian approaches to non-adiabatic molecular dynamics, in *Quantum Chemistry and Dynamics of Excited States: Methods and Applications* (Wiley Online Library, Hoboken, New Jersey, 2020), pp. 563–594.
- [89] R. Requist and E. K. U. Gross, Exact Factorization-Based Density Functional Theory of Electrons and Nuclei, *Phys. Rev. Lett.* **117**, 193001 (2016).
- [90] J. P. Perdew, K. Burke, and M. Ernzerhof, Generalized Gradient Approximation Made Simple, *Phys. Rev. Lett.* **77**, 3865 (1996).
- [91] C. Shepard, R. Zhou, D. C. Yost, Y. Yao, and Y. Kanai, Simulating electronic excitation and dynamics with real-time propagation approach to TDDFT within plane-wave pseudopotential formulation, *J. Chem. Phys.* **155**, 100901 (2021).